

# A parallel algorithm for the enumeration of benzenoid hydrocarbons

**Iwan Jensen**

Department of Mathematics and Statistics, The University of Melbourne, Vic. 3010, Australia

E-mail: [I.Jensen@ms.unimelb.edu.au](mailto:I.Jensen@ms.unimelb.edu.au)

Received 19 September 2008

Accepted 21 January 2009

Published 27 February 2009

Online at [stacks.iop.org/JSTAT/2009/P02065](http://stacks.iop.org/JSTAT/2009/P02065)

[doi:10.1088/1742-5468/2009/02/P02065](https://doi.org/10.1088/1742-5468/2009/02/P02065)

**Abstract.** We present an improved parallel algorithm for the enumeration of fixed benzenoids  $B_h$  containing  $h$  hexagonal cells. We can thus extend the enumeration of  $B_h$  from the previous best  $h = 35$  up to  $h = 50$ . Analysis of the associated generating function confirms to a very high degree of certainty that  $B_h \sim A\kappa^h/h$  and we estimate that the growth constant  $\kappa = 5.161\,930\,154(8)$  and the amplitude  $A = 0.280\,8499(1)$ .

**Keywords:** critical exponents and amplitudes (theory), series expansions

**ArXiv ePrint:** [0808.0963](https://arxiv.org/abs/0808.0963)

---

**Contents**

|   |           |
|---|-----------|
| <b>1. Introduction</b>                  | <b>2</b>  |
| <b>2. Computer algorithm</b>            | <b>3</b>  |
| 2.1. Finite lattice algorithm . . . . . | 3         |
| 2.2. Parallelization . . . . .          | 8         |
| <b>3. Numerical analysis</b>            | <b>11</b> |
| <b>Acknowledgments</b>                  | <b>14</b> |
| <b>References</b>                       | <b>15</b> |

---

**1. Introduction**

A benzenoid or planar polyhex is a special type of hydrocarbon molecule. Its hexagonal system is obtained by deleting all carbon–hydrogen bonds, leaving clusters of hexagons joined at an edge (a carbon–carbon bond). They thus appear as clusters of identical hexagons in the plane. The interiors of the clusters are filled with hexagons so there are no internal holes. These structures have appeared independently in the chemical and mathematical literature. In the mathematics literature they are discussed as self-avoiding polygons on the hexagonal lattice [1] and a distinction is made between fixed and free embeddings. Fixed polygons are considered distinct up to a translation while free polygons are considered equivalent under translations, rotations and reflections. Polygons are typically enumerated according to their perimeter or area. In the chemistry literature the number of free polygons [2] has been universally considered. The number of benzenoids or planar polyhexes is equal to the number of free hexagonal self-avoiding polygons enumerated by area.

The enumeration of the number  $b_h$  of benzenoids of  $h$  cells remains an important topic in computational and theoretical chemistry. The monograph by Gutman and Cyvin [2] provides a comprehensive review of all aspects. Until a few years ago progress was slow and incremental as calculations were based on direct counting of benzenoids. As the number of these grows as  $b_h \sim \kappa^h$ , where the growth constant  $\kappa \simeq 5.16$ , it is clear that to obtain one further term one needs more than five times the computing power. Up to 1989, the number of benzenoids up to  $h = 12$  was known [2]. Ten years later this had been improved to  $h = 21$  [3], while more recently, the number of benzenoids up to  $h = 24$  was obtained [4]. In 2002 [5] a major breakthrough was obtained using a different type of algorithm that enabled the number of *fixed* benzenoids  $B_h$  to be enumerated for  $h \leq 35$  and  $b_h$  was then obtained to the same size by using direct counting algorithms to enumerate benzenoids possessing certain symmetries, e.g. they may be symmetric with respect to an axis of reflection or certain rotations. For direct counting algorithms the CPU time taken to enumerate  $B_h$  grows as  $\kappa^h$ , whereas for our algorithm time consumption grows approximately as  $1.65^h$ ; since  $1.65 < \kappa \simeq 5.16$  we may say that the new algorithm is exponentially faster than direct counting. Its drawbacks are that it is much more memory

intensive (memory grows exponentially with  $h$ ) than direct counting, for which memory requirements are negligible, as well as being much more difficult to implement.

In [5] it was shown that there exists a growth constant  $\kappa$  such that

$$\lim_{h \rightarrow \infty} B_h^{1/h} = \kappa \quad (1)$$

and the universally accepted, but as yet unproved, conjecture

$$B_h \sim A\kappa^h h^\theta \quad \text{as } h \rightarrow \infty \quad (2)$$

for the asymptotic form for  $B_h$  was confirmed to a high degree of certainty. It is widely accepted that for models such as benzenoids, other self-avoiding polygon models enumerated by area and polyominoes (or lattice animals) the exponent  $\theta$  is given by the Lee–Yang edge singularity exponent [6] and thus  $\theta = -1$  for benzenoids. Numerical analysis [5] confirmed this conjecture to a very high degree of certitude and yielded the estimate  $\kappa = 5.161\,930\,16(8)$  for the growth constant and  $A = 0.280\,8491(1)$  for the critical amplitude.

In this paper we describe an efficient parallel version of the algorithm used in [5] and extend the count for fixed benzenoids up to  $h = 50$ . We do not attempt to count  $b_h$  since asymptotically  $B_h = 12b_h$  so any results regarding the asymptotic behaviour of  $B_h$  and  $b_h$  are essentially the same (and the ratio of the two sequences  $B_h/b_h$  converges rapidly to its asymptotic limit as evidenced by the fact that  $12 - B_{35}/b_{35} \simeq 1.355 \times 10^{-10}$ ). Furthermore the direct counting algorithms for benzenoids with a symmetry have computational complexity  $\lambda^h$  where  $\lambda = \kappa^{1/k}$  if enumerating benzenoids with a  $k$ -fold symmetry, so in the worst case we have  $\lambda = \sqrt{\kappa} \simeq 2.27$ , which is a much worse asymptotic growth than that achieved with the algorithm for fixed benzenoids. Our analysis of the extended data yields the even more precise estimates  $\kappa = 5.161\,930\,154(8)$  and a revised estimate for the critical amplitude  $A = 0.280\,8499(1)$ .

## 2. Computer algorithm

A detailed description of the original computer algorithm can be found in [5]. For this work we use a slightly different algorithm and we have therefore chosen to describe it in some detail below before specifying how it can be turned into an efficient parallel algorithm.

### 2.1. Finite lattice algorithm

We count the number of fixed benzenoids using the so-called finite lattice method pioneered by Enting [7]. In this method the number of benzenoids is obtained by calculating the contributions from benzenoids contained within finite sub-lattices. As in [1, 5] we embed the hexagonal lattice in the square lattice as the brickwork lattice (see figure 1) and our finite lattices are rectangles of width  $W$  and length  $L$ . The minimum number of cells needed to span a rectangle from top to bottom and left to right is essentially  $W + \max(0, L - (W + 1)/2)$  (simply note that a single ‘line’ of cells starting in the top left corner and going down the diagonal contains  $W$  cells and extends  $(W + 1)/2$  cells to the right). So benzenoids up to a maximal size  $h_{\max}$  can be counted by combining the counts from all finite  $W \times L$  lattices with  $W + \max(0, L - (W + 1)/2) \leq h_{\max}$ .

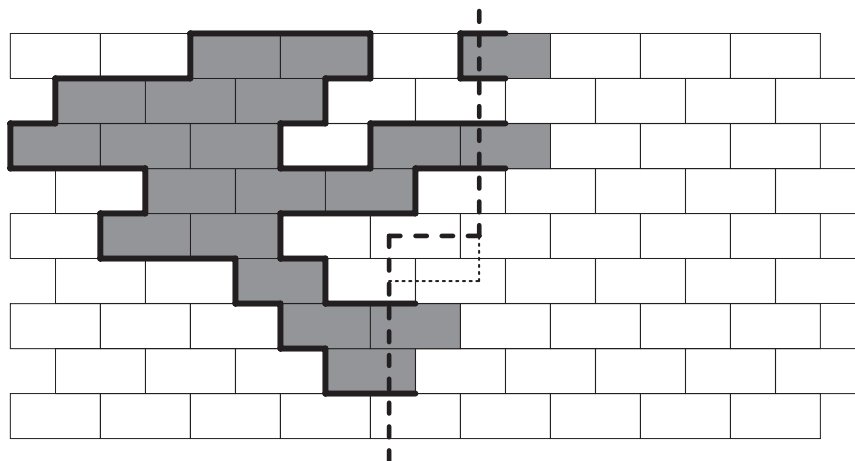


**Figure 1.** A snapshot of the boundary line (dashed line) during the transfer-matrix calculation on the brickwork lattice. Benzenoids are enumerated by successive moves of the kink in the boundary line, as exemplified by the position given by the dotted line, so that two vertices at a time are added to the rectangle. To the left of the boundary line we have drawn (shaded cells) an example of a partially completed benzenoid.

The number of benzenoids in a given rectangle is calculated using transfer-matrix techniques. The transfer-matrix (TM) technique involves drawing a boundary line through the rectangle intersecting a set of up to  $W + 1$  edges. Benzenoids in a given rectangle are enumerated by moving the boundary line so as to add two vertices (or a single cell) at a time as shown in figure 1. In this fashion we build up the rectangle column by column with each column built up cell by cell. As we move the boundary line it intersects partially completed benzenoids consisting of disjoint loops that must all be connected to form a single benzenoid. This TM algorithm is used for rectangles where  $L \geq W$ . Note that the hexagonal lattice (or bricklayer lattice) is not symmetric with respect to rotation. So for rectangles with  $L < W$  we choose instead to let the boundary line cut across  $L + 1$  edges in the lengthwise direction and we then move the boundary line from the bottom to the top of the rectangle. This ensures that the number of edges cut by the boundary line is minimal and at most  $2h_{\max}/3$ . The TM algorithms in the two cases are essentially identical and differ only in ‘surface’ effects. Below we give some further details of the TM algorithm.

To avoid situations leading to graphs with more than a single component we have to forbid a loop from closing on itself if the boundary line intersects any other loops. So two loop-ends can only be joined if they belong to different loops or all other edges are empty. To exclude loops which close on themselves we need to label the occupied edges in such a way that we can easily determine whether or not two loop-ends belong to the same loop. The most obvious choice would be to give each loop a unique label. However, on two-dimensional lattices there is a more compact scheme relying on the fact that two loops can never intertwine. Each end of a loop is assigned one of two labels depending on whether it is the lower end or the upper end of a loop. Each configuration along the boundary line can thus be represented by a set of edge states or a state vector  $s = \{\sigma_i\}$ ,

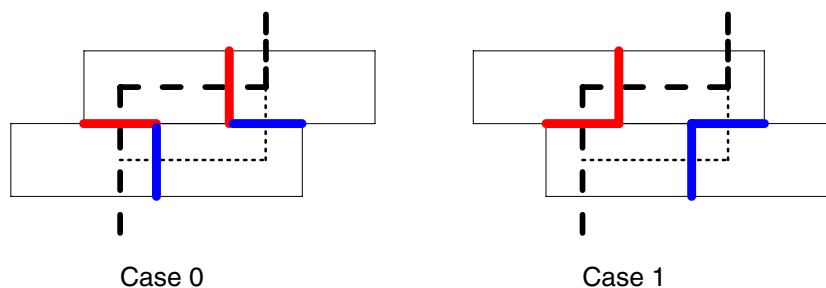


**Figure 2.** The two different update cases encountered in the move of the TM boundary line. Red (blue) edges indicate the kink edges before (after) the move.

where

$$\sigma_i = \begin{cases} 0 & \text{empty edge,} \\ 1 & \text{lower end of a loop,} \\ 2 & \text{upper end of a loop.} \end{cases} \quad (3)$$

With this encoding the state along the boundary line in figure 1 is  $s = \{01\ 010\ 002\ 212\}$ . It is easy to see that this encoding uniquely describes which loop-ends are connected. In order to find the upper loop-end, matching a given lower end, we start at the lower end and work upwards in the configuration counting the number of ‘1’s and ‘2’s that we pass (the ‘1’ of the initial lower end is *not* included in the count). We stop when the number of ‘2’s exceeds the number of ‘1’s. This ‘2’ marks the matching upper end of the loop.

When the boundary line is moved we encounter two different cases as we add a new cell as illustrated in figure 2. When building up a new column we alternate between the two cases. For each configuration of occupied or empty edges along the boundary, we maintain a generating function for partially completed benzenoids. The generating function is a (truncated) polynomial  $p_s(q)$ , where  $s$  is the state vector specifying the ‘source’ configuration. When the boundary line is moved, a given state vector  $s$  is transformed into two new state ‘target’ vectors  $t_1$  and  $t_2$  and  $q^{k_1}p_s(q)$  is added to  $p_{t_1}(q)$  and  $q^{k_2}p_s(q)$  is added to  $p_{t_2}(q)$ , where  $k_1$  and  $k_2$  are 1 or 0 depending on whether the new cell is part of the benzenoid or not. It is quite simple to determine whether a newly added unit cell belongs to a benzenoid or not. Moving through a configuration we note that as we reach the first occupied edge we pass from the outside to the inside of a benzenoid, the next occupied edge takes us to the outside again, and so on. In this fashion all unit cells intersected by the boundary line are uniquely assigned to the interior or exterior of a benzenoid.

In figures 3 and 4 we illustrate the possible new configurations of the edges in the kink of the boundary line as we add a new cell. The actual update rules will depend not only on the number of occupied kink edges in the input configuration but also on their states. The update rules are summarized in table 1 and a few comments are in order. The first five rows should be self-explanatory. In rows 6 and 9 overlining of the output state means that we have connected two lower (upper) loop-ends and we therefore have to relabel one of the matching upper (lower) loop-ends in the target state as a lower (upper) state. The matching loop-ends are easily located as explained below (3). In row 7 Acc means accumulate into final count for  $B_h$  if valid. Here we are forming a closed loop and

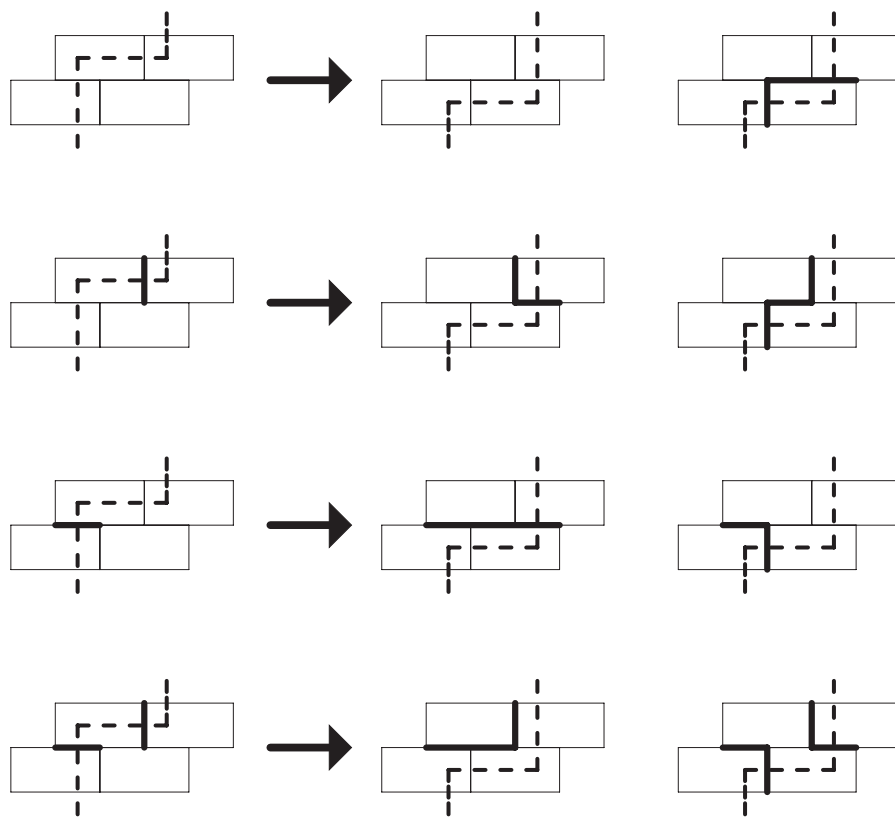


**Figure 3.** The possible updates in Case 0 when the input state (leftmost column) has zero, one or two occupied edges. The rightmost column shows the possible outputs.

**Table 1.** Update rules for Case 0 and Case 1.

| Case 0 |                     | Case 1 |        |                     |                     |
|--------|---------------------|--------|--------|---------------------|---------------------|
| Input  | Output              | Input  | Output |                     |                     |
| '00'   | '00'                | '12'   | '00'   | '00'                | '12'                |
| '01'   | '01'                | '10'   | '01'   | '01'                | '10'                |
| '02'   | '02'                | '20'   | '02'   | '02'                | '20'                |
| '10'   | '01'                | '10'   | '10'   | '01'                | '10'                |
| '20'   | '02'                | '20'   | '20'   | '02'                | '20'                |
| '11'   | ' $\overline{00}$ ' | '11'   | '11'   | ' $\overline{00}$ ' | ' $\overline{12}$ ' |
| '12'   | Acc                 | '12'   | '12'   | Acc                 | —                   |
| '21'   | '00'                | '21'   | '21'   | '00'                | '12'                |
| '22'   | ' $\overline{00}$ ' | '22'   | '22'   | ' $\overline{00}$ ' | ' $\overline{12}$ ' |

this is only allowed if there are no other occupied edges in the state (otherwise we either produce graphs with several separate components or interior holes, neither of which are permissible benzenoids). In Case 1 row 7 the second output can never occur. Finally in row 8 we connect upper and lower loop-ends from two different loops. This is always allowed and the output states need no further comments.

A major improvement to the basic method can be obtained by using the approach first adopted in [8]. As stated earlier we require valid benzenoids to span the rectangle in

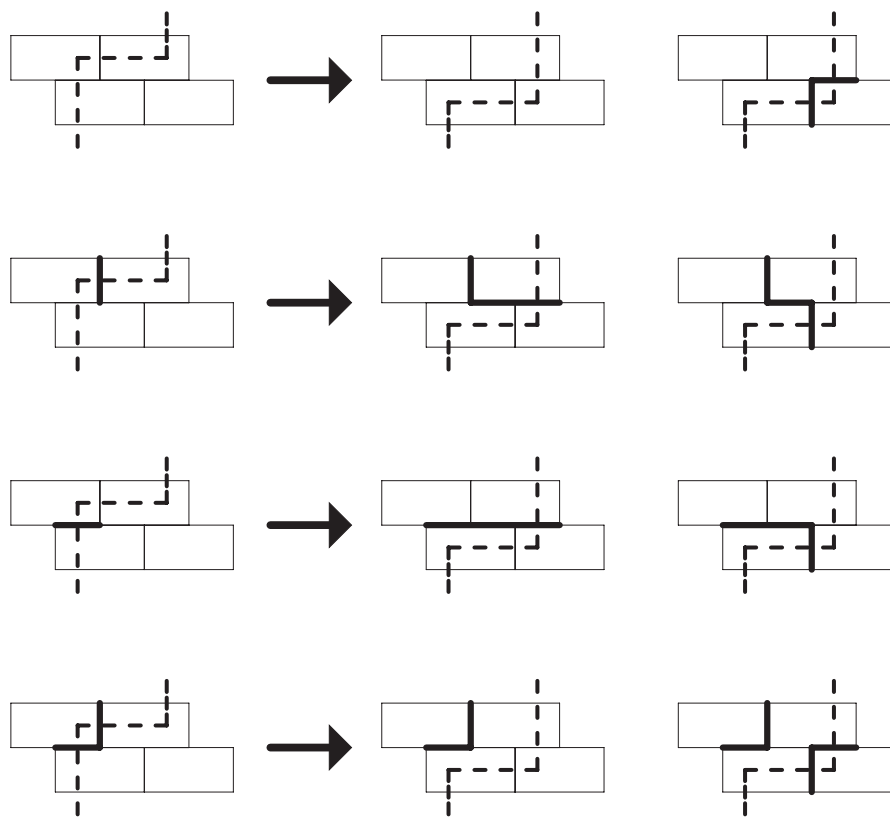


Figure 4. Similar to figure 3 but for Case 1.

both directions. In other words we directly enumerate benzenoids of width exactly  $W$  and length  $L$ . To implement the TM algorithm efficiently we use several memory and time saving methods. The most important is what we call *pruning*. This procedure, details of which are given in [8], allows us to discard most of the possible configurations for large  $W$  because they only contribute to benzenoids of size greater than  $h_{\max}$ . Briefly this works as follows. For each configuration we keep track of the current minimum number of cells  $h_{\text{cur}}$  already inserted to the left of the boundary line. We then calculate the minimum number of additional cells  $h_{\text{add}}$  required to produce a valid benzenoid. There are three contributions, namely the number of cells required to close the benzenoid, the number of cells needed (if any) to ensure that the benzenoid touches both the lower and upper border, and finally the number of cells needed (if any) to extend at least  $W$  cells in the lengthwise direction (remember that we are looking at rectangles with  $L \geq W$ ). If the sum  $h_{\text{cur}} + h_{\text{add}} > h_{\max}$  we can discard the partial generating function for that configuration, and of course the configuration itself, because it would not make a contribution to the benzenoid count up to the size that we are trying to obtain.

Those familiar with algebraic languages will recognize that each configuration of labelled loop-ends forms a Motzkin word [9]. It is known that the number of Motzkin words of length  $m$  grows like  $3^m$ . The maximal number of bonds intersected by the boundary line grows as  $2h_{\max}/3$ . This implies that the complexity of enumerating benzenoids of size  $h$  grows as  $3^{2h/3} \simeq 2.08^h$ , multiplied by some polynomial in  $h$ . Thus the basic transfer-matrix approach already provides a dramatic improvement over direct enumeration algorithms,

**Table 2.** Number of fixed benzenoids  $B_h$  of size  $h \geq 36$ .

| $h$ | $B_h$  |
|-----|--|
| 36  | 352 506 828 543 839 738 006 802              |
| 37  | 1 771 125 269 041 561 567 830 953            |
| 38  | 8 905 113 919 188 230 264 955 009            |
| 39  | 44 804 571 829 235 959 198 699 855           |
| 40  | 225 570 974 088 699 920 561 748 746          |
| 41  | 1 136 340 745 302 289 809 680 018 862        |
| 42  | 5 727 773 558 054 438 208 070 950 886        |
| 43  | 28 887 056 504 374 868 913 302 241 736       |
| 44  | 145 763 914 212 751 560 334 802 981 991      |
| 45  | 735 894 997 233 174 457 602 406 978 869      |
| 46  | 3 716 988 842 355 112 053 567 240 722 854    |
| 47  | 18 783 102 592 560 998 779 533 576 292 617   |
| 48  | 94 958 908 613 774 943 408 509 332 060 260   |
| 49  | 480 273 434 248 924 455 452 231 252 618 009  |
| 50  | 2430 068 453 031 180 290 203 185 942 420 933 |

which have complexity  $5.16^h$ . With the further improvements outlined above, it is not possible to give a theoretical analysis of the computational complexity of the algorithm, but an empirical analysis in [5] suggested that the improvements reduce the complexity to  $\lambda^h$  with  $\lambda \simeq 1.65$ . For this work a slight further improvement has been obtained reducing  $\lambda$  to 1.56 or so. In addition some further memory saving strategies were adopted. The effectiveness of these can be gauged by noting that in [5] the calculation of  $B_h$  up to  $h = 35$  required some 5 Gb of memory and we can now achieve a similar task using only some 250 Mb of memory.

The integers  $B_h$  become very large and exceed  $2^{64}$  which causes overflow when using 64 bit integers. The solution to this problem is use modular arithmetic and do the calculation modulo several numbers  $p_i$  and then reconstruct the true  $B_h$  using the Chinese remainder theorem [10]. In our case it sufficed to do the calculations modulo  $p_0 = 2^{62}$  and  $p_1 = 2^{62} - 1$ . It should be noted that the computationally expensive part of our algorithm is pruning. Compared to this the time taken to perform the modular calculations updating the partial generating functions is insignificant. Since the calculations were done on a shared facility, CPU time was more at a premium than memory and we did the calculation using both  $p_0$  and  $p_1$  in a single run. The total CPU time expended on the calculations was approximately 22 000 CPU hours.

In table 2 we list the 15 additional terms for  $B_h$  with  $h \geq 36$  obtained in this work; the original 35 terms can be found in [5] or downloaded from our web-site [13].

## 2.2. Parallelization

The computational complexity of the FLM grows exponentially with the number of terms that one wishes to calculate. It is therefore little wonder that implementations of the algorithms have always been geared towards using the most powerful computers available. By now parallel computing is well established as the paradigm for high performance computing and in particular cluster computing has emerged as the dominant platform for

large scale computing facilities. The transfer-matrix algorithms used in the calculations of the finite lattice contributions are eminently suited for parallel computations.

The most basic concern for any efficient parallel algorithm is to minimize the communication between processors and ensure that each processor does roughly the same amount of work and use similar amounts of memory. In practice one naturally has to strike some compromise and accept a certain degree of variation across the processors.

One of the main ways of achieving a good parallel algorithm using data decomposition is to try to find an invariant under the operation of the updating rules. That is, we seek to find some property of the configurations along the boundary line which does not change in a single iteration. The algorithm for the enumeration of benzenoids is quite complicated since not all possible configurations occur due to pruning and an update at a given set of edges might change the state of an edge far removed, e.g., when two lower loop-ends are joined we have to relabel one of the associated upper loop-ends as a lower loop-end in the new configuration. However, there is still an invariant since any edge not directly involved in the update cannot change from being empty to being occupied and vice versa. That is, only the edges at the kink of the boundary line can change their occupation status. This invariant allows us to parallelize the algorithm in such a way that we can do the calculation completely independently on each processor with just two redistributions of the data set each time an extra column is added to the lattice.

The main points of the algorithm are summarized below:

- (1) With the boundary line straight (having no kinks) distribute the configurations and their generating functions across processors so that configurations with the same occupation pattern along the *lower* half of the boundary line are placed on the same processor.
- (2) Do the TM update inserting the top half of a new column. This can be done *independently* by each processor because the occupation pattern in the lower half remains unchanged.
- (3) Upon reaching the halfway mark redistribute the data so that configurations with the same occupation pattern along the *upper* half of the boundary line are placed on the same processor.
- (4) Do the TM update inserting the bottom half of a new column.
- (5) Go back to 1.

The redistribution among processors was done as follows:

- (1) On each processor run through the configurations to establish the occupation pattern (in the lower or upper half of the boundary)  $c$  of each configuration and calculate  $n(c)$ , the number of configurations with a given pattern.
- (2) Calculate the *global* sum of  $n(c)$ .
- (3) Sort the global sum  $n(c)$ .
- (4) Assign each pattern to a processor  $p_i$  as follows:
  - (a) Set  $p_i = 0$ .
  - (b) Assign the *most* frequent unassigned pattern  $c$  to processor  $p_i$ .

**Table 3.** Number of processors with total CPU time and actual running time (in the format hh:mm) as well and memory use for the parallel algorithm for enumerating benzenoids of maximal size 43 at width 22.

| Proc. | Total time | Run time | Max Conf    | Min Conf   | Max Term    | Min Term    |
|-------|------------|----------|-------------|------------|-------------|-------------|
| 1     | 60:13      | 60:20    | 107 350 066 |            | 207 111 142 |             |
| 2     | 61:53      | 30:59    | 52 982 622  | 52 435 395 | 102 711 198 | 102 666 398 |
| 4     | 62:28      | 15:38    | 26 389 619  | 26 183 924 | 51 559 593  | 51 025 667  |
| 8     | 63:17      | 7:55     | 13 289 367  | 13 078 219 | 26 179 885  | 25 492 182  |
| 16    | 69:28      | 4:22     | 6 725 270   | 6 486 246  | 13 245 615  | 12 717 598  |
| 32    | 69:05      | 2:10     | 3 440 269   | 3 274 193  | 6 871 820   | 6 347 966   |
| 64    | 71:33      | 1:08     | 1 768 626   | 1 616 220  | 3 839 775   | 3 191 842   |

- (c) If the number of configurations assigned to  $p_i$  is less than the number of configurations assigned to processor 0 then assign the *least* frequent unassigned patterns to  $p_i$  until the desired inequality is achieved.
- (d) Set  $p_i = (p_i + 1) \bmod N_p$ , where  $N_p$  is the number of processors.
- (e) Repeat from (b) until all patterns have been assigned.
- (5) On each processor run through the configurations sending each configuration to its assigned processor.

The bulk of the calculations were performed on the facilities of the Australian Partnership for Advanced Computing (APAC). The APAC facility is an SGI Altix cluster with 1920 1.6 GHz Itanium2 processors grouped into 30 partitions with 64 processors each. The cluster has a total peak speed over 11 Tflops. Nodes are connected via a SGI's NUMalink with a latency  $< 2 \mu\text{s}$  (MPI) and bandwidth of  $3.2 \text{ Gb s}^{-1}$  bidirectional. We used up to 128 processors per run using a maximum of 230 Gb of memory and 22000 CPU hours.

In table 3 we have listed the time and memory use of the algorithm for  $h_{\max} = 43$  at  $W = 22$  using from 1 to 64 processors. The memory use of the single-processor job was about 3 Gb. Firstly, we look at the issue of balancing the memory use of the parallel algorithm. By design we are attempting to balance this to the greatest extent possible since in a cluster environment memory is often the most crucially constrained resource. This aspect is examined via the numbers in columns 4–7. At any given time during the calculation each processor handles a subset of the total number of configurations. For each processor we monitor the maximal numbers of configurations and terms retained in the generating functions. The balancing can be roughly gauged by looking at the largest (Max Conf) and smallest (Min Conf) maximum numbers of configurations handled by individual processors during the execution of the program. In columns 6 and 7 are listed the largest (Max Term) and smallest (Min Term) numbers of terms retained in the generating functions associated with the subset of configurations. As can be seen, the algorithm is quite well balanced. Even with 64 processors, where each processor uses only about 50 Mb of memory, the difference between the processor handling the maximal and minimal number of configurations is less than 10%. For the total number of terms retained in the generating functions the difference is less than 20%. So our aim of balancing memory use has clearly been achieved.

The next issue is that of balancing the CPU time used by the algorithm. As can be seen, the algorithm scales reasonable well from 1 to 64 processors since the total combined CPU time (column 2; the format is hours:minutes) used by all processors increases only by about 10%. Likewise the run time (column 3; the format is hours:minutes:seconds) of the program is approximately halved when the number of processors is doubled. This is not quite as good a scaling as was achieved for some previous algorithms [11, 12] where the total CPU time stayed constant. The main reason for the discrepancy is that the time-consuming part of our algorithm is the pruning. For ‘simpler’ problems on the square lattice it turned out that the time consumption was fairly constant irrespective of the occupation pattern. Pruning benzenoid configurations is more complicated<sup>1</sup>. In our previous work [11, 12] the CPU time used in communication tasks never exceeded 10% of the total. However, for benzenoids a simple timing of the various routines shows that as much as 30% of the time was used in communication tasks. We believe that most of the additional time use is due to ‘latency’, that is the task of redistributing the data among processors that must complete before further processing can be done. The redistribution is thus blocking. If certain subsets of configurations sitting on processor  $p_j$  take a long time to process they can thus lead to imbalances where other processors must wait for the completion of the calculation on processor  $p_j$ . Unfortunately it is not possible to determine *a priori* whether a certain set of configurations with a particular occupation pattern are ‘slow’. However, this does suggest that there is some room for improvement to the redistribution, perhaps by including additional information (say which borders have been touched or the total number of occupied edges) so as to further sub-divide the set of configurations, thus making it easier to balance the workload. Another option would be to monitor the time used to process each configuration and use this as part of the information used in the redistribution. However, this should not come at the cost of unbalanced memory use. These possibilities remain to be explored in future work.

### 3. Numerical analysis

From the coefficients  $B_h$  we have the first 50 terms in the respective generating function,

$$G(q) = \sum_h B_h q^h \sim A(q)(1 - \kappa q)^{-1-\theta} \quad (4)$$

where the functional form of the generating follows from (2) with the radius of convergence of the generating function given by  $q_c = 1/\kappa$ . In order to obtain the singularity structure of the generating function we used the numerical method of differential approximants [14]. Very briefly, in this method we approximate the generating function by the solution to a linear, inhomogeneous, ordinary differential equation (ODE) with polynomial coefficients. The singular behaviour of such ODEs is a well known classical mathematics problem (see e.g. [15]) and the singular points and exponents are easily calculated. Even if the function *globally* is not a solution of a such a linear ODE (as is the case for SAP) one hopes that *locally* in the vicinity of the (physical) critical points the generating function can still be well approximated by a solution to a linear ODE.

<sup>1</sup> We do not give details here but just note that on the square lattice the three contributions to  $h_{\text{add}}$  essentially decouple and can be determined more or less independently. This is no longer the case on the hexagonal lattice, vastly complicating the pruning.

**Table 4.** Estimates for the critical point  $q_c = 1/\kappa$  and critical exponent  $-1 - \theta$  as obtained from second- and third-order differential approximants with  $L$  being the degree of the inhomogeneous polynomial.

| $L$ | Second-order approximants |                   | Third-order approximants |                   |
|-----|---------------------------|-------------------|--------------------------|-------------------|
|     | $q_c = 1/\kappa$          | $-1 - \theta$     | $q_c = 1/\kappa$         | $-1 - \theta$     |
| 0   | 0.193 725 984 74(16)      | -0.000 001 36(87) | 0.193 725 984 40(23)     | -0.000 000 55(37) |
| 2   | 0.193 725 984 48(24)      | -0.000 000 77(43) | 0.193 725 984 286(90)    | -0.000 000 36(16) |
| 4   | 0.193 725 984 40(11)      | -0.000 000 56(42) | 0.193 725 984 36(22)     | -0.000 000 51(39) |
| 6   | 0.193 725 984 43(27)      | -0.000 000 68(51) | 0.193 725 984 16(16)     | -0.000 000 09(41) |
| 8   | 0.193 725 984 41(32)      | -0.000 000 52(93) | 0.193 725 984 182(83)    | -0.000 000 13(21) |
| 10  | 0.193 725 984 44(19)      | -0.000 000 69(38) | 0.193 725 984 205(94)    | -0.000 000 20(23) |

A  $K$ th-order differential approximant (DA) to a function  $F(x)$  is formed by matching the coefficients in the polynomials  $Q_i(x)$  and  $P(x)$  of degree  $N_i$  and  $L$ , respectively, so that one of the formal solutions to the inhomogeneous differential equation

$$\sum_{i=0}^K Q_i(x) \left( x \frac{d}{dx} \right)^i \tilde{F}(x) = P(x) \quad (5)$$

agrees with the first  $M = L + \sum_i (N_i + 1)$  series coefficients of  $F$ . We normalize the DA by setting  $Q_K(0) = 1$ , thus leaving us with  $M$  rather than  $M + 1$  unknown coefficients. The singularities of  $F(x)$  are thus approximated by zeros  $x_i$  of  $Q_K(x)$  and the associated critical exponent  $\lambda_i$  is estimated from the associated indicial equation [15].

One can increase the degree of the polynomials and the order of the underlying differential equation until there are no more known coefficients. For each specific choice of order and degrees one must then solve a set of linear equation for the coefficients in the polynomials in the approximating ODE. A substantial number of such differential approximants are constructed, and a statistical procedure is used to estimate the critical point and critical exponent. All calculations were carried out using floating point arithmetic with quadruple precision (our algorithm has been tested extensively using Maple with a precision of 100 digits and this revealed that rounding errors are not an issue).

In table 4 we have listed estimates for the critical point  $q_c = 1/\kappa$  and critical exponent  $-1 - \theta$  obtained from a differential approximant analysis [14]. The estimates were obtained by averaging over many individual approximants using a procedure (see [16] for details) which automatically discards any spurious outlying approximants. Each approximant used at least 42 terms of the series and the degree of the inhomogeneous polynomial was varied from  $L = 0$  to 10. Taken together, the estimates are consistent with the conjectured exact value  $\theta = -1$  for the critical exponent, while for the critical point we obtain  $q_c = 0.193\,725\,9843(3)$  or for the growth constant  $\kappa = 5.161\,930\,154(8)$ .

While the estimates listed in table 4 are very accurate, one issue which always arises in a differential approximant analysis is the possibility of systematic bias. In particular it is possible that the estimates have not yet converged to their true asymptotic values. In order to address this possibility we plot in figure 5 individual estimates for the critical point  $q_c$  and critical exponent  $-1 - \theta$  as a function of the maximal size or number of terms

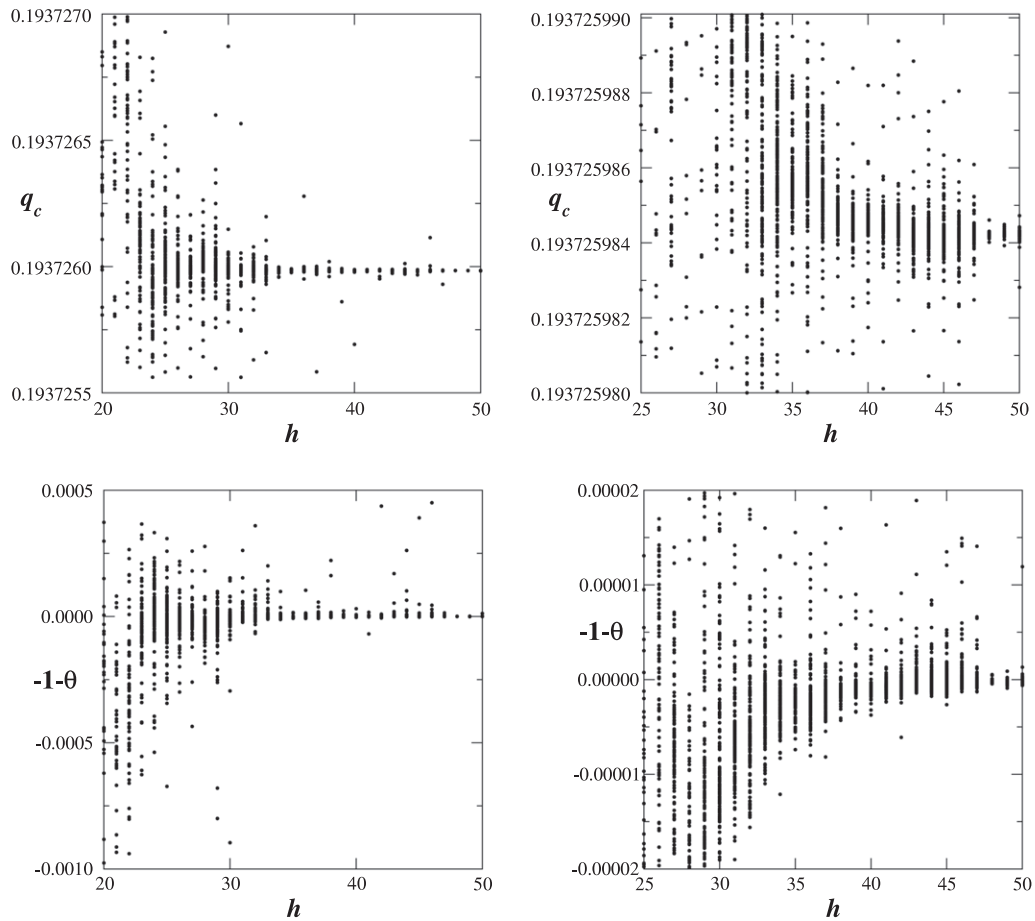


**Figure 5.** Estimates for the critical point  $q_c$  (top panels) and critical exponent  $-1 - \theta$  (bottom panels) versus the maximal size  $h$  (or number of terms) used in the differential approximant analysis. Each dot represents a data point obtained from a third-order approximant with  $L = 0, 2, \dots, 10$ . The left panels show a view of most approximants while the right panels are a more detailed view at the data for high values of  $h$ .

$h$  used to form the differential approximant. From this figure it is clear that the estimates do settle down to very well defined values. There is no sign of any systematic drift in the estimates for  $h > 40$  or so. In particular the conclusion that  $\theta = -1$  exactly appears to be completely safe. Likewise the estimates for  $q_c$  settle down to a value in full agreement with the estimate  $q_c = 0.1937259843(3)$  from above.

Now that the exact value of  $\theta$  has been confirmed and an accurate estimate for  $\kappa$  obtained we turn our attention to the ‘fine structure’ of the asymptotic form of the coefficients. In particular we are interested in obtaining accurate estimates for the leading critical amplitude  $A$ . Our method of analysis consists in fitting the coefficients to an assumed asymptotic form. The asymptotic form (2) for the coefficients  $B_h$  only explicitly gives the leading contribution. In general one would expect corrections to scaling given by a set of correction-to-scaling exponents. We have argued elsewhere [17] and found in the previous study [5] that there is no sign of non-analytic correction-to-scaling exponents.

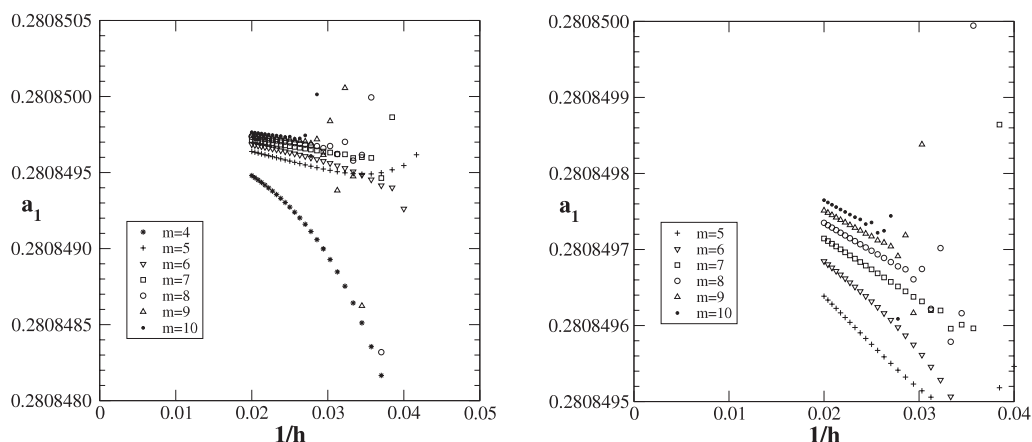


**Figure 6.** Estimates for the leading amplitude  $a_1$  versus  $1/h$  where  $h$  is the maximal size used in the fit to the asymptotic form (6) for the coefficients  $B_h$ . The plot in the right panel is a more detailed view of the data in the left panel.

The upshot of this is that  $B_h$  follows the asymptotic form

$$B_h = \kappa^h \left[ a_1/h + a_2/h^2 + a_3/h^3 + \dots + O(\exp(-h)) \right]. \quad (6)$$

We then obtain estimates for  $a_1 = A$  by fitting  $B_h$  to this form. That is we truncate (6) after  $m$  terms, take a sub-sequence of coefficients  $\{B_h, B_{h-1}, \dots, B_{h-m+1}\}$ , plug into the formula above and solve the resulting  $m$  linear equations to obtain estimates for the amplitudes. It is then advantageous to plot estimates for the leading amplitude  $a_1$  against  $1/h$  for several values of  $m$ . The results are plotted in the left panel of figure 6. We clearly have very well behaved estimates. In the right panel we take a more detailed look at the data and from this plot we estimate that  $a_1 = 0.2808499(1)$ . In a similar manner we estimate that  $a_2 = -0.14518(2)$ . The following amplitudes  $a_k, k \geq 3$ , show quite a lot of curvature (and some even appear to diverge). This would indicate that the asymptotic form (6) is in fact not quite correct and thus that our previous conclusion that there is no sign of non-analytic correction-to-scaling exponents may well be incorrect (at least for this problem). We tried to include other ad hoc terms (such as half-integer exponents) but none of these improved the convergence and essentially they had no effect of the estimate for  $a_1$ . The conclusion to our experimentation is that we are certain that the first two terms of (6) are correct, but beyond this more terms with non-integer exponents are likely to occur though we do not as yet have a clear idea of the possible values of these non-analytic correction-to-scaling exponents.

## Acknowledgments

The calculations presented in this paper would not have been possible without a generous grant of computer time on the server cluster of the Australian Partnership for Advanced Computing (APAC). We also used the computational resources of the Victorian Partnership for Advanced Computing (VPAC). We gratefully acknowledge financial support from the Australian Research Council.

## References

- [1] Enting I G and Guttmann A J, 1989 *J. Phys. A: Math. Gen.* **22** 1371
- [2] Gutman I and Cyvin S, 1989 *Introduction to the Theory of Benzenoid Hydrocarbons* (Berlin: Springer)
- [3] Caporossi G and Hansen P, 1998 *J. Chem. Inf. Comput. Sci.* **38** 610
- [4] Brinkmann G, Caporossi G and Hansen P, 2001 *Commun. Math. Chem.* **43** 133
- [5] Vöge M, Guttmann A J and Jensen I, 2002 *J. Chem. Inf. Comput. Sci.* **42** 456
- [6] Parisi G and Sourlas N, 1981 *Phys. Rev. Lett.* **46** 871
- [7] Enting I G, 1980 *J. Phys. A: Math. Gen.* **13** 3713
- [8] Jensen I and Guttmann A J, 1999 *J. Phys. A: Math. Gen.* **32** 4867
- [9] Delest M P and Viennot G, 1984 *Theor. Comput. Sci.* **34** 169
- [10] Knuth D E, 1997 *Seminumerical Algorithms. The Art of Computer Programming* 3rd edn, vol 2 (Reading, MA: Addison-Wesley)
- [11] Jensen I, 2003 *J. Phys. A: Math. Gen.* **36** 5731
- [12] Jensen I, 2003 *Computational Science—ICCS 2003 (Springer Lecture Notes in Computer Science vol 2659)* ed P M A Sloot, D Abramson, A V Bogdanov, J J Dongarra, A Y Zomaya and Y E Gorbachev (Berlin: Springer) pp 203–12
- [13] Jensen I, <http://www.ms.unimelb.edu.au/~iwan/>
- [14] Guttmann A J, 1989 *Phase Transitions and Critical Phenomena* vol 13, ed C Domb and J L Lebowitz (New York: Academic) pp 1–234
- [15] Ince E L, 1927 *Ordinary Differential Equations* (London: Longmans Green)
- [16] Jensen I, 2006 *J. Phys.: Conf. Ser.* **42** 163
- [17] Jensen I and Guttmann A J, 2000 *J. Phys. A: Math. Gen.* **33** L257